



UNIVERSITÀ
DI TORINO

Characterization of Hadronic Showers in the Belle II Electromagnetic Calorimeter

Emanuele Zanusso

Dipartimento di Fisica
Università degli Studi di Torino

January 14, 2026

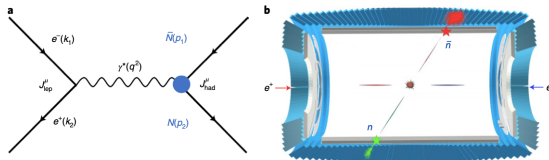
Outline

- 1. Anti-neutrons in physics experiments**
- 2. Study via signal Monte Carlo sample**
- 3. Study of Monte Carlo cocktail**
- 4. Outlook**

Anti-neutron in HEP experiments

The \bar{n} plays a key role in several physics measurements, such as:

- The neutron e.m. form factor studies in $e^+ + e^- \rightarrow n + \bar{n}$ process



- Some decay channels studied at B-factories which involve \bar{n}
 1. The hyperons decay channel:
$$\bar{\Lambda}^0 \rightarrow \pi^0 + \bar{n}, \quad \bar{\Sigma}^- \rightarrow \pi^- + \bar{n}, \quad \bar{\Lambda}_c \rightarrow K_s^0 + \pi^0 + \bar{n}$$
- Discrimination between other neutral particles (γ) and \bar{n}

Anti-neutrons in astrophysics

The \bar{n} also plays a key role in several astrophysics measurements, such as:

- Studying \bar{n} - anti-hyperon potential to improve the understanding of the equation of state of the neutron stars
- Investigating dark matter through anti-deuterons (\bar{D}) in cosmic rays, produced by dark matter annihilation or decay

$A_{d.m.} + B_{d.m.} \rightarrow \text{hadrons } (n, \bar{n}, p, \bar{p} \text{ etc...})$

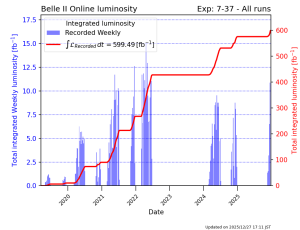
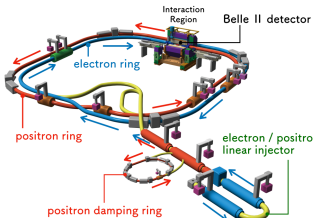
$X_{d.m.} \rightarrow \text{hadrons } (n, \bar{n}, p, \bar{p} \text{ etc...})$

\bar{D} is mainly produced through a coalescence mechanism $\bar{n} + \bar{p} \rightarrow \bar{D}$,
where \bar{p} and \bar{n} are nearby in the phase-space

The Belle II experiment

SuperKEKB is an asymmetric $e^+ e^-$ collider (Tsukuba, Japan)

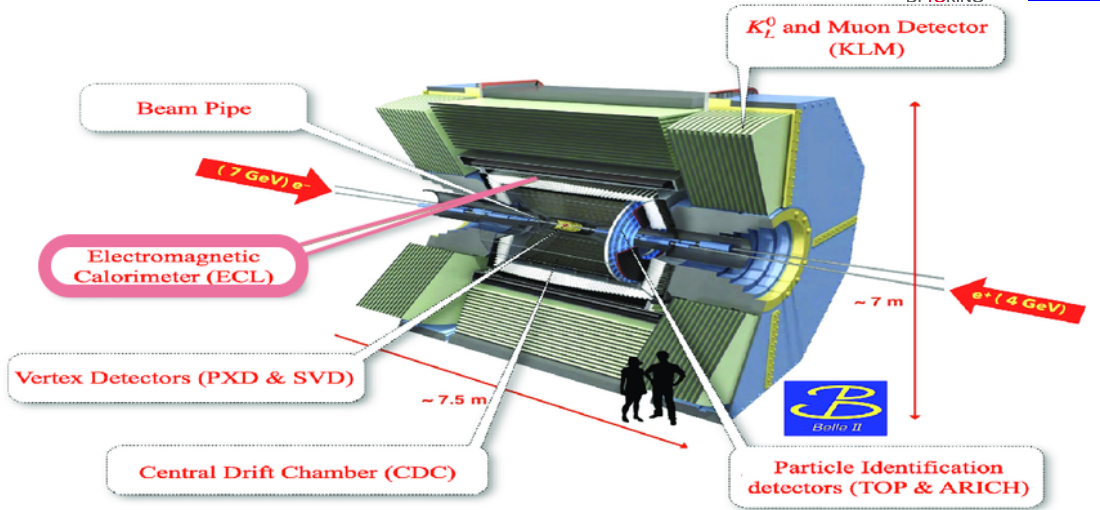
- 7 GeV electron beam (HER)
- 4 GeV positron beam (LER)
- Peak Luminosity $\sim 5.1 \times 10^{34} cm^{-2}s^{-1}$
- Design Luminosity $\sim 8 \times 10^{35} cm^{-2}s^{-1}$
→ x40 the Belle's one



It operates mainly around $\Upsilon(4S)$ resonance (~ 10.58 GeV):

- This resonance decays almost exclusively into entangled couples of $B\bar{B} \rightarrow B$ -factory
- Several goals: flavour physics, BSM physics, heavy hadrons spectroscopy etc...

The Belle II experiment

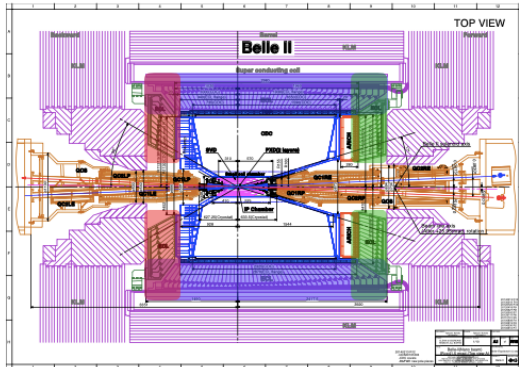


The Electromagnetic Calorimeter

The ECL plays a central role in this thesis

- Array of **CsI(Tl)** crystals (8376 $6 \times 6 \times 30 \text{ cm}^3$ crystals in total)
- It covers barrel and end-cap regions ($12^\circ \leq \theta \leq 155^\circ$)
- Energy resolution of 4% @100 MeV and 1.6% @8 GeV

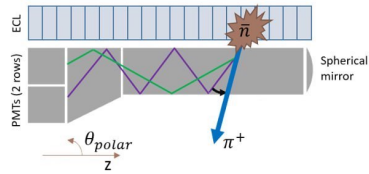
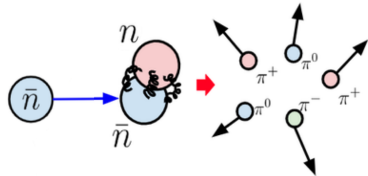
Barrel
FWD endcap
BWD endcap



Anti-neutron interactions in physics

The \bar{n} interacts primarily via strong nuclear force, producing hadronic showers
It can annihilate with nucleons in the ECL, producing light mesons (mainly pions)

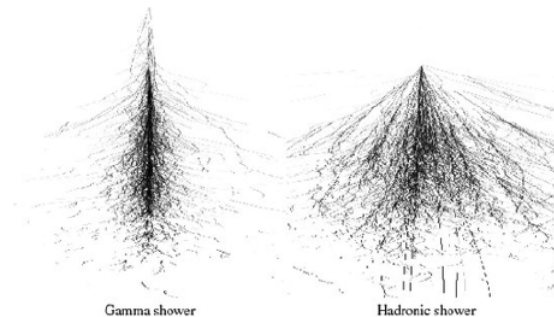
- π^0 decays into $\gamma\gamma$, producing electromagnetic showers that are fully contained in the ECL
- π^\pm undergo hadronic interactions, which are not fully contained in the ECL → both the forward (KLM) and backward (TOP) directions are involved



Electromagnetic and hadronic showers

Different processes occur for electromagnetic and hadronic showers:

1. Bremsstrahlung and pair production process (e^+, e^-, γ) and $\pi^0 \rightarrow \gamma\gamma$
 2. Strong interactions of hadrons with the material ($p, n, pions, kaons...$)
-
- About the 95% of the hadronic shower is contained within a cylinder of radius λ_{had} (~ 44.12 cm in CsI(Tl))
 - About the 90% of the e.m. shower is contained within a cylinder of radius R_M (~ 3.6 cm in CsI(Tl))



The MANTRA project (PRIN2022)



Measuring Anti-Neutron: Tagging and Reconstruction Algorithm

- A general method to measure the $E_{\bar{n}}$ up to 10 GeV, by combining information from:
 1. A detector with high time resolution (TOP)
 2. An electromagnetic calorimeter (**ECL**)
 3. A muon system (KLM)
- These features are common in modern general-purpose collider experiments such as **Belle II** and BESIII, which do not have a dedicated calorimeter
- For MANTRA project, only signals from ECL and TOP are taken into account. In this thesis only ECL signals are studied

Are \bar{n} hadronic showers correctly simulated in the Belle II software?

The MANTRA project

Anti-neutrons cannot be reconstructed by sub-detectors.

The measurement of the energy is a two-step process:

1. \bar{n} identification via its induced ECL clusters (study of the shower shape)
2. Combine the signals from TOP and ECL to reconstruct the \bar{n} energy, in cases of backscattering or pre-showering
 - If only π^0 are produced ($\sim 5\%$), the energy is all contained in the calorimeter, the shower is fully reconstructed
 - Otherwise ($\sim 95\%$): the products may escape the crystals
→ the goal is to complement the calorimeter information with that from the adjacent detectors

Preliminary concept

Several channels can be selected to look at \bar{n} annihilations, such as:

- $e^+ + e^- \rightarrow p + \bar{n} + \pi^- + (\gamma_{ISR})$ (Mine)
- $\bar{\Lambda}_c \rightarrow K_s^0 + \pi^0 + \bar{n}$
- $\Lambda(\rightarrow p + \pi^-) + \bar{\Lambda}(\rightarrow \bar{n} + \pi^0)$

Several variables can be used to validate the showers shape for \bar{n} identification, such as:

- **Zernike Moments** (backup)
- **Lateral momentum** defined as: $C_{LM} = \frac{\sum_{i=2}^n \omega_i E_i r_i^2}{\omega_0 E_0 r_0^2 + \omega_1 E_1 r_1^2 + \sum_{i=2}^n \omega_i E_i r_i^2}$
- **Second moment** defined as: $C_{SM} = \frac{\sum_{i=0}^n \omega_i E_i r_i^2}{\sum_{i=0}^n \omega_i E_i}$

Analysis outline

1. Study of the selected signal channel $e^+ + e^- \rightarrow p + \bar{n} + \pi^- + (\gamma_{ISR})$
 - (a) Recoil identification from the system $p + \pi^-$ (with and without ISR)
 - (b) Study of the kinematic recoil variables (momentum, angles, energy, etc...)
 - (c) Study of the effect of 1C kinematic fit over the recoil mass
 - (d) Study of ECL shower shape variables
2. Study of MC cocktail sample:
 - (a) Recoil identification from the system $p + \pi^-$ (with and without ISR)
 - (b) Study of the kinematic recoil variables (momentum, angles, energy, etc...)
3. Study of real data sample:
 - (a) Recoil identification from the system $p + \pi^-$ (with and without ISR)
 - (b) Constraint with 1C kinematic fit over the recoil mass
 - (c) Examine Data/MC agreement in ECL cluster shapes from \bar{n} channel

Analysis outline (1)

- The analyzed channel is:

$$e^+ + e^- \rightarrow p + \bar{n} + \pi^- + (\gamma_{ISR})$$

The reconstructed particles are (cuts and selections in the next slide):

- (a) $p + \pi^- + (\gamma_{ISR})$ which compose the recoil system
- (b) Neutral clusters associated to \bar{n} candidates list used to compare its variables with those of the recoil

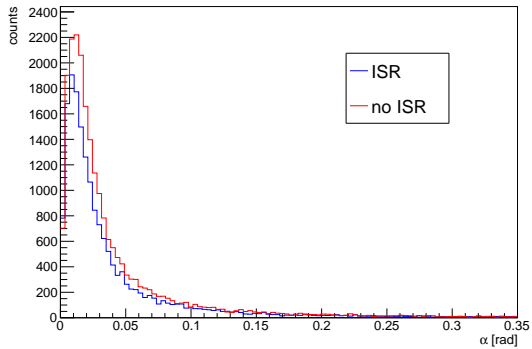
rowNo	decay tree	decay final state	iDcyTr	nEtr	nCEtr
1	$vpho \rightarrow \pi^- \bar{n} p$	$\pi^- \bar{n} p \gamma^F \gamma^F$	0	35291	35291
2	$e^+ e^- \rightarrow vpho \gamma^I \gamma^I, vpho \rightarrow \pi^- \bar{n} p$	$\pi^- \bar{n} p \gamma^I \gamma^I$	2	22971	58262
3	$e^+ e^- \rightarrow vpho \gamma^I, vpho \rightarrow \pi^- \bar{n} p$	$\pi^- \bar{n} p \gamma^I$	1	18735	76997
4	$vpho \rightarrow \pi^- \bar{n} p \gamma^F$	$\pi^- \bar{n} p \gamma^F$	3	10005	87002
5	$e^+ e^- \rightarrow vpho \gamma^I \gamma^I, vpho \rightarrow \pi^- \bar{n} p \gamma^F$	$\pi^- \bar{n} p \gamma^I \gamma^I \gamma^F$	6	5274	92276
6	$e^+ e^- \rightarrow vpho \gamma^I, vpho \rightarrow \pi^- \bar{n} p \gamma^F$	$\pi^- \bar{n} p \gamma^I \gamma^F$	4	4621	96897
7	$vpho \rightarrow \pi^- \bar{n} p \gamma^F \gamma^F$	$\pi^- \bar{n} p \gamma^F \gamma^F$	7	1503	98400
8	$e^+ e^- \rightarrow vpho \gamma^I \gamma^I, vpho \rightarrow \pi^- \bar{n} p \gamma^F \gamma^F$	$\pi^- \bar{n} p \gamma^I \gamma^I \gamma^F \gamma^F$	8	700	99100
9	$e^+ e^- \rightarrow vpho \gamma^I, vpho \rightarrow \pi^- \bar{n} p \gamma^F \gamma^F$	$\pi^- \bar{n} p \gamma^I \gamma^F \gamma^F$	5	597	99697
10	$vpho \rightarrow \pi^- \bar{n} p \gamma^F \gamma^F \gamma^F$	$\pi^- \bar{n} p \gamma^F \gamma^F \gamma^F$	9	167	99864
11	$e^+ e^- \rightarrow vpho \gamma^I, vpho \rightarrow \pi^- \bar{n} p \gamma^F \gamma^F \gamma^F$	$\pi^- \bar{n} p \gamma^I \gamma^F \gamma^F \gamma^F$	12	63	99927
12	$e^+ e^- \rightarrow vpho \gamma^I \gamma^I, vpho \rightarrow \pi^- \bar{n} p \gamma^F \gamma^F \gamma^F$	$\pi^- \bar{n} p \gamma^I \gamma^I \gamma^F \gamma^F \gamma^F$	10	61	99988
13	$e^+ e^- \rightarrow vpho \gamma^I, vpho \rightarrow \pi^- \bar{n} p \gamma^F \gamma^F \gamma^F \gamma^F$	$\pi^- \bar{n} p \gamma^I \gamma^F \gamma^F \gamma^F \gamma^F$	11	4	99992
14	$e^+ e^- \rightarrow vpho \gamma^I \gamma^I, vpho \rightarrow \pi^- \bar{n} p \gamma^F \gamma^F \gamma^F \gamma^F$	$\pi^- \bar{n} p \gamma^I \gamma^I \gamma^F \gamma^F \gamma^F \gamma^F$	15	4	99996
15	$vpho \rightarrow \pi^- \bar{n} p \gamma^F \gamma^F \gamma^F \gamma^F$	$\pi^- \bar{n} p \gamma^F \gamma^F \gamma^F \gamma^F$	14	2	99998
16	$vpho \rightarrow \pi^- \bar{n} p \gamma^F \gamma^F \gamma^F \gamma^F \gamma^F$	$\pi^- \bar{n} p \gamma^F \gamma^F \gamma^F \gamma^F \gamma^F$	13	1	99999
17	$e^+ e^- \rightarrow vpho \gamma^I \gamma^I, vpho \rightarrow \pi^- \bar{n} p \gamma^F \gamma^F \gamma^F \gamma^F \gamma^F$	$\pi^- \bar{n} p \gamma^I \gamma^I \gamma^F \gamma^F \gamma^F \gamma^F$	16	1	100000

- 100k events.** The reconstruction efficiency is:

$$\epsilon = \frac{n^{\circ} \text{ of reconstructed candidates}}{n^{\circ} \text{ of generated events}} \sim 22\%(18\%)$$

Applied selections and cuts

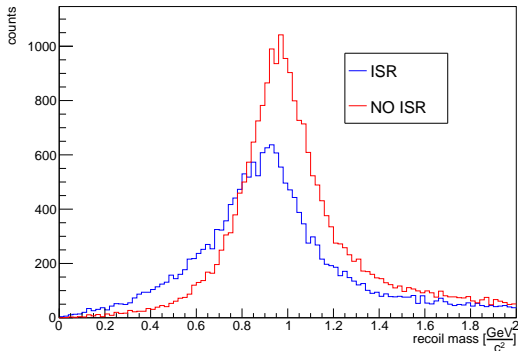
- (a) **proton**: standard PID selection, with tracks required to originate from the IP
- (b) **pion**: standard PID selection
- (c) **anti-neutron**: neutral clusters from ECL
- (d) $0 \text{ GeV} < \text{recoil mass} < 2 \text{ GeV}$
- (e) $\alpha < 0.35 \text{ rad} (\sim 20 \text{ deg})$



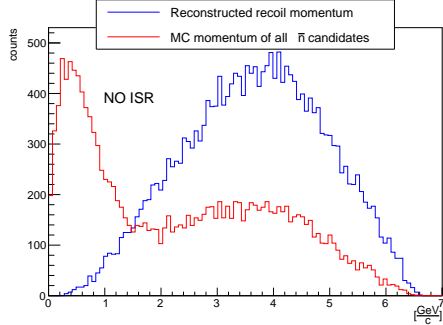
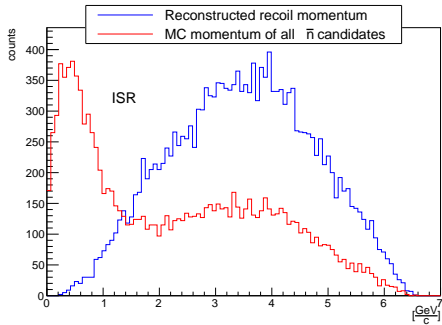
Where α is the angle between the recoil vector direction and the closest \bar{n} cluster

The recoil mass

- The recoil mass is well reconstructed in both ISR (p, π^-, γ_{ISR}) and no ISR (p, π^-) cases
 - Variables associated with the \bar{n} candidate clusters can be compared with the reconstructed recoil variables (p, θ)
- Since there is more than one γ_{ISR} per event, the  distribution shows a higher number of entries in the left tail



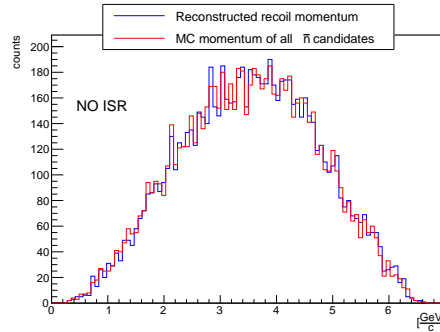
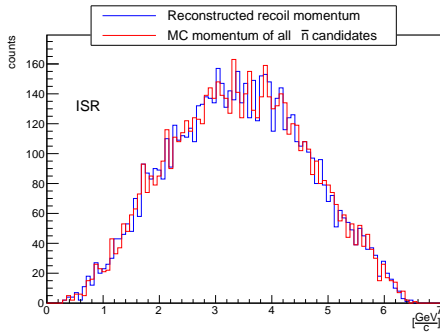
The recoil and the \bar{n} momentum



- The \bar{n} candidate list shows a discrepancy with the recoil momentum
 - (a) Could **cluster split-off** and/or **pre-showering** introduce the left peak?
 - (b) **Do they affect MC association too?**

The recoil and the \bar{n} momentum

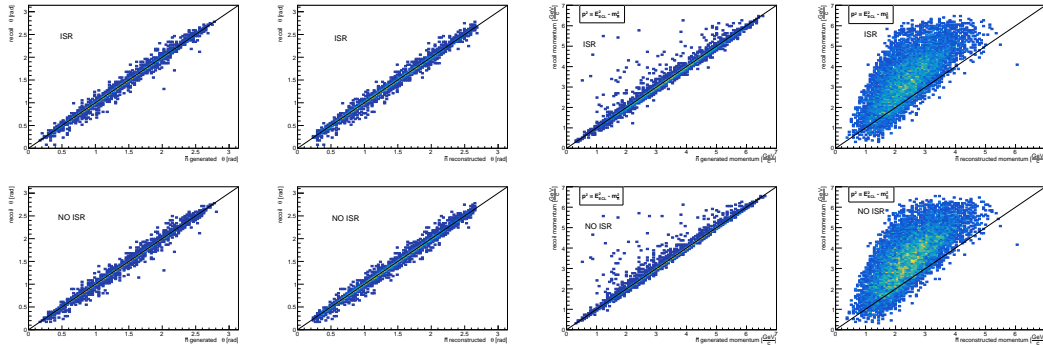
- MC truth can be imposed by selecting only correctly reconstructed \bar{n} candidates from the \bar{n} list
- A good correspondence can be observed between the two distributions, in both the ISR and NO ISR cases



\bar{n} vs recoil vector correlation



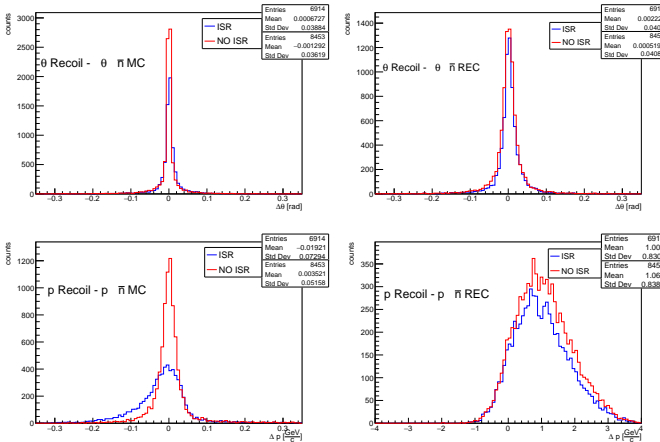
UNIVERSITÀ
DI TORINO



- Poor resolution is observed in reconstructed \bar{n} momentum ($p_{rec}^2 = E_{ECL}^2 - m_{\bar{n}}^2$), in both the ISR and NO ISR cases

\bar{n} vs recoil vector residuals

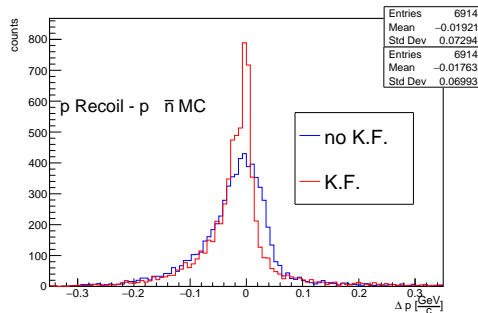
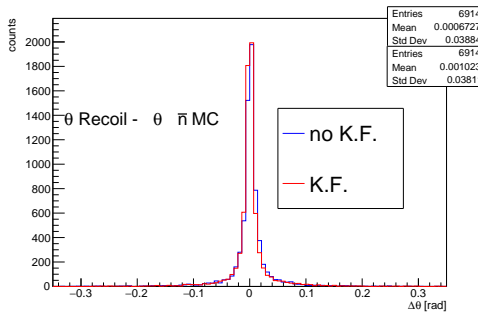
- Good correlation is observed at the generator level in both the momentum and θ distributions
- Besides exhibiting poor resolution, the reconstructed momentum of the \bar{n} is underestimated
→ missing energy in the shower



Kinematic Fit over the recoil mass

A 1C kinematic fit can possibly be used to add a constraint and improve the recoil resolution:

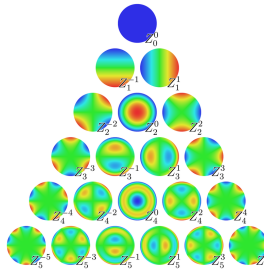
- No significant differences can be seen in θ_{recoil} vs MC $\theta_{\bar{n}}$
- An improvement can be observed in p_{recoil} vs MC $p_{\bar{n}}$



\bar{n} ECL cluster variables

The aim is to validate several \bar{n} shower shapes variables, such as:

- **Energy** of the cluster
- **E1E9** and **E9E21**
- **Zernike Moments**



10	11	12	13	14
25	2	3	4	15
24	9	1	5	16
23	8	7	6	17
22	21	20	19	18

- **Lateral momentum** and **Second moment** defined as:

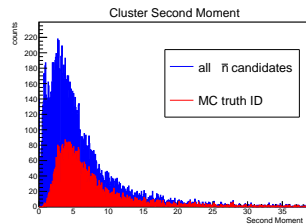
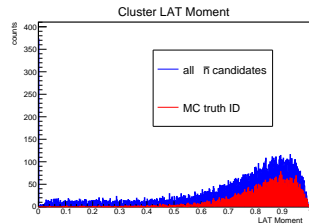
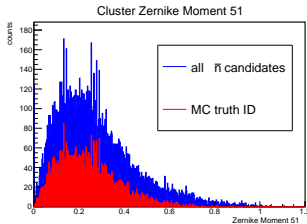
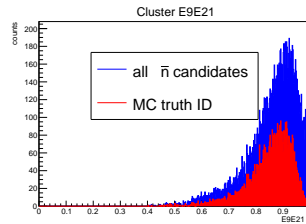
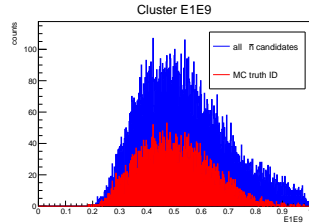
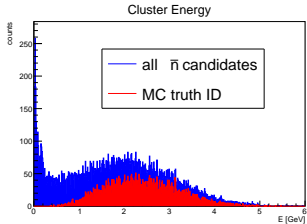
$$C_{LM} = \frac{\sum_{i=2}^n \omega_i E_i r_i^2}{\omega_0 E_0 r_0^2 + \omega_1 E_1 r_1^2 + \sum_{i=2}^n \omega_i E_i r_i^2}$$

$$C_{SM} = \frac{\sum_{i=0}^n \omega_i E_i r_i^2}{\sum_{i=0}^n \omega_i E_i}$$

\bar{n} ECL cluster variables

all \bar{n} candidates

\bar{n} MC truth ID

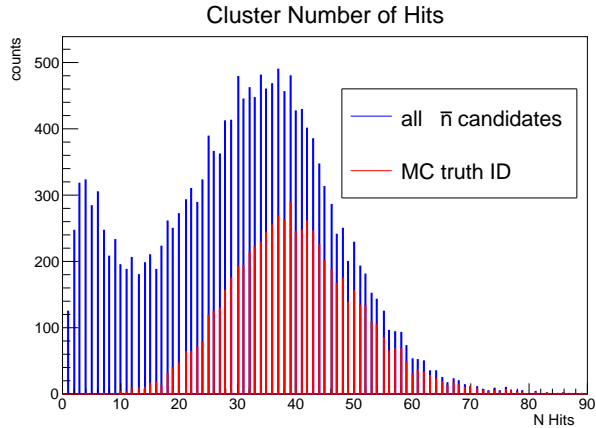


\bar{n} ECL cluster variables

1. Could secondary clusters (split-off) be mis-identified as \bar{n} primary cluster, during reconstruction?
2. Could it be a wrong association due to pre-showering in the TOP detector?

→ further studies can be addressed with a particle gun generator

\bar{n} clusters mainly involve 15 or more crystals



Summary (1)

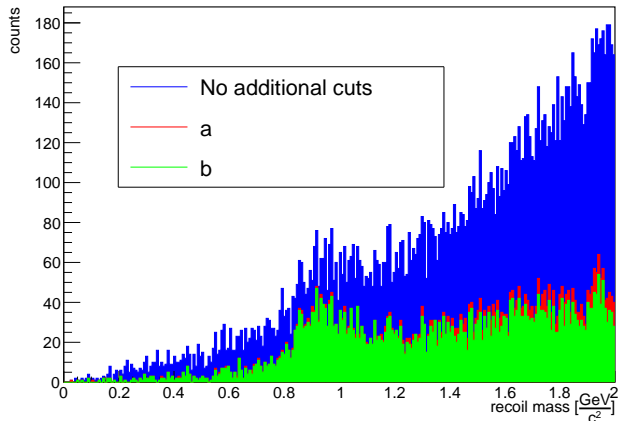
- Channel $e^+ + e^- \rightarrow p + \bar{n} + \pi^- + (\gamma_{ISR})$ has been studied and recoil system is correctly reconstructed from the secondary background
- Reconstructed \bar{n} variables, such as momentum and shower-shape variables, should be further investigated. This could be due to:
 - (a) Cluster split-offs with the ECL and pre-showering occurring within the TOP may affect the shower shape variables
 - (b) An incorrect Monte Carlo association could also influence these variables
 - This could be studied by testing the ECL response with a \bar{n} particle gun generator
- 1C kinematic fit can be possibly adopted during MC/Data comparison, in order to improve the recoil resolution

Analysis outline (2)

- Study of cocktail using the following MC sample:
 $q\bar{q}$ cocktail with 341 M events (Luminosity: 215 fb^{-1})
- Only the p and π^- are used to build the recoil vector (NO ISR for the moment) →
Can the signal be correctly reconstructed among the other cocktail channels?
- Following selections have been applied:
 1. Real particles ID selection on p and π^- from the MC truth
 2. $0 \text{ GeV} < \text{recoil mass} < 2 \text{ GeV}$
 3. The best candidate is selected via α (closest candidate)
- Same strategy as before:
 - (a) Identify the signal peak near the \bar{n} mass ($\sim 0.939 \text{ GeV}$) adding further cuts
 - (b) Study the shower shape variables in a selected recoil mass region, replacing the MC truth selections with data driven ones
 - (c) Compare it with data (Data/MC agreement)

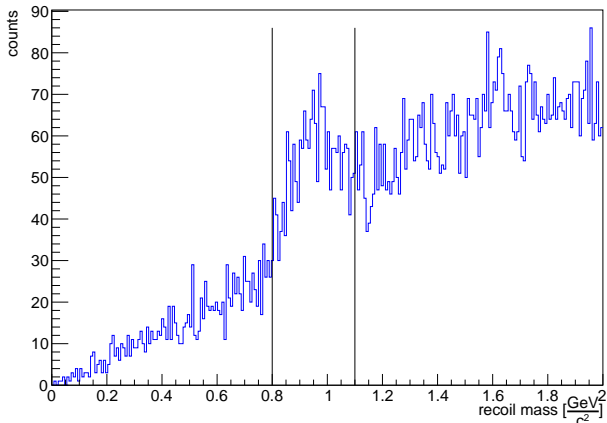
Recoil mass distribution - MC selections

- The following cuts are applied to enhance the signal:
 - No additional charged tracks in the event █
 - No additional charged tracks in the event and $\alpha < 0.35$ rad (angular cut on the closest candidate) █
- A peak can be observed above the \bar{n} mass → **the signal is correctly selected in the MC cocktail**

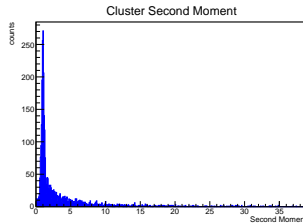
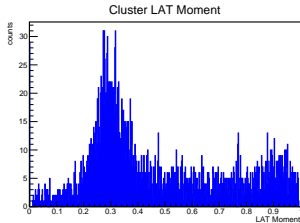
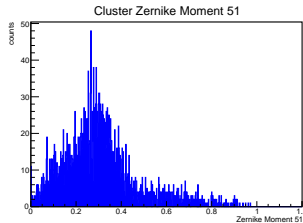
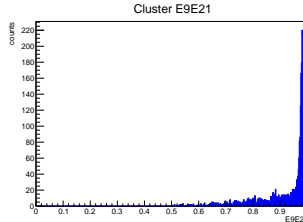
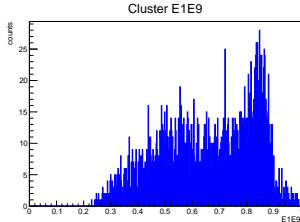
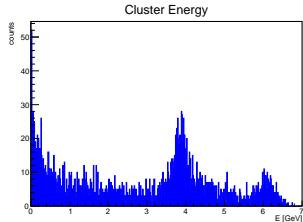


Recoil mass distribution - Real cuts

- "Real cuts" can be applied instead of MC truth selections, such as:
 - (a) **proton**: standard PID selection, with tracks required to originate from the IP
 - (b) **pion**: standard PID selection
- To select the signal, a recoil mass cut in the range (0.8-1.1) GeV can be applied to study the shower shapes variables



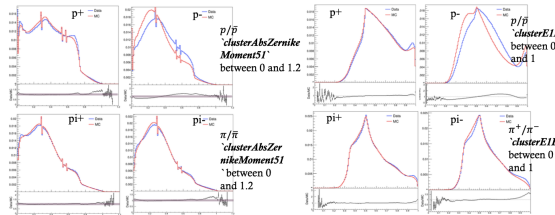
\bar{n} ECL cluster variables



Summary (2)

- Study of $q\bar{q}$ cocktail has been performed
- The recoil mass is correctly reconstructed using both Monte Carlo based selections and data-driven cuts, in the presence of other cocktail channels
- A further selection on the recoil mass has been applied in order to study the shower shape variables and then validate it in a Data/MC agreement

Analysis of a $\Lambda \rightarrow p + \pi^-$ ($\bar{\Lambda} \rightarrow \bar{p} + \pi^+$) sample shows that:



Poor Data/MC agreement in $\bar{p} \rightarrow$ will it be the same for \bar{n} ?

Outlook

The following topics will be faced from today:

1. Study of the Monte Carlo software association and of cluster split-off effects in the ECL using a particle gun
2. Study the entire cocktail production, adding further collections
3. Study of the Data/MC agreement of the shower-shape variables using the evaluated real selections



UNIVERSITÀ
DI TORINO

Thank you for your attention

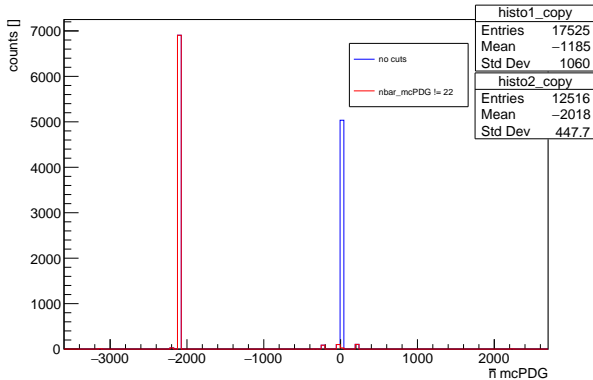
Emanuele Zanuso

Dipartimento di Fisica
Università degli Studi di Torino

January 14, 2026

\bar{n} mcPDG I

γ 's are mis-identified as \bar{n} in reconstruction:



UNIVERSITÀ
DI TORINO

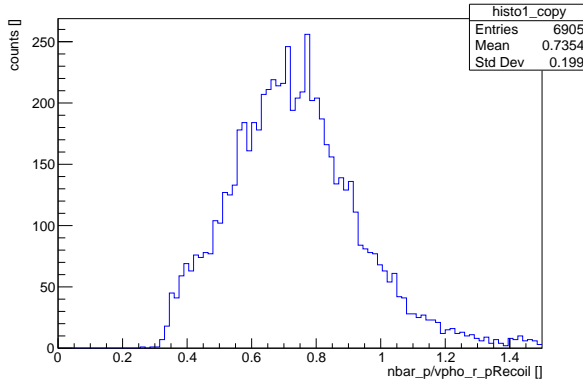


$p_{\bar{n}}/\text{pRecoil}$ |

\bar{n} is underrated in the most of cases (annihilation process + loss of energy)



UNIVERSITÀ
DI TORINO



Recommended PID selections I

PID probability defined as:

protonID

[\[source\]](#)

proton identification probability defined as $\mathcal{L}_p / (\mathcal{L}_e + \mathcal{L}_\mu + \mathcal{L}_\pi + \mathcal{L}_K + \mathcal{L}_p + \mathcal{L}_d)$, using info from all available detectors

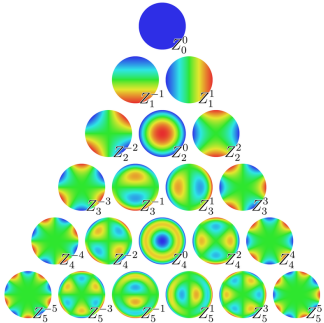
pionID

[\[source\]](#)

pion identification probability defined as $\mathcal{L}_\pi / (\mathcal{L}_e + \mathcal{L}_\mu + \mathcal{L}_\pi + \mathcal{L}_K + \mathcal{L}_p + \mathcal{L}_d)$, using info from all available detectors

Zernike Moments I

- Zernike polynomials are widely used as basis functions of image moments



Ci sono polinomi di Zernike [pari e dispari](#). Quelli pari sono definiti come:

$$Z_n^m(\rho, \varphi) = R_n^m(\rho) \cos(m\varphi)$$

e quelli dispari come:

$$Z_n^{-m}(\rho, \varphi) = R_n^m(\rho) \sin(m\varphi)$$

dove m e n sono [numeri interi non negativi](#) con $n \geq m$, ϕ è l'[angolo azimutale](#), ρ è la distanza radiale $0 \leq \rho \leq 1$ e R_n^m sono i polinomi radiali definiti di seguito. I polinomi di Zernike hanno la proprietà di essere limitati a un intervallo da -1 a +1, cioè $|Z_n^m(\rho, \varphi)| \leq 1$. I polinomi radiali R_n^m sono definiti come:

$$R_n^m(\rho) = \sum_{k=0}^{\frac{n-m}{2}} \frac{(-1)^k (n-k)!}{k! (\frac{n+m}{2} - k)! (\frac{n-m}{2} - k)!} \rho^{n-2k}$$

per $n - m$ pari e sono identicamente zero per $n - m$ dispari.